Article:
Ai, Q, Ke, D, Zuo, J et al. (4 more authors) (2020) High-Order Model-Free Adaptive Iterative Learning Control of Pneumatic Artificial Muscle With Enhanced Convergence. IEEE Transactions on Industrial Electronics, 67 (11). pp. 9548-9559. ISSN 0278-0046

https://doi.org/10.1109/tie.2019.2952810

High-Order Model-Free Adaptive Iterative Learning Control of Pneumatic Artificial Muscle with Enhanced Convergence

Qingsong Ai, *Member, IEEE*, Da Ke, Jie Zuo, Wei Meng, *Member, IEEE*, Quan Liu
Zhiqiang Zhang and Sheng Q. Xie, *Senior Member, IEEE*

***Abstract*—Pneumatic artificial muscles (PAMs) have been widely used in actuation of medical devices due to their intrinsic compliance and high power to weight ratio features. However, the nonlinearity and time-varying nature of PAMs makes it challenging to maintain high-performance tracking control. In this paper, a High-Order Pseudo-Partial Derivative based Model-Free Adaptive Iterative Learning Controller (HOPPD-MFAILC) is proposed to achieve fast convergence speed. The dynamics of PAM is converted into a dynamic linearization model during iterations, meanwhile, a high-order estimation algorithm is designed to estimate the pseudo-partial derivative component of the linearization model by only utilizing the input and output data in previous iterations. The stability and convergence performance of the controller is verified through theoretical analysis. Simulation and experimental results on PAM demonstrate that the proposed HOPPD-MFAILC can track the desired trajectory with improved convergence and tracking performance.**

***Index Terms*—Pneumatic artificial muscle, model-free adaptive control, iterative learning control, convergence.**

I. Introduction

PNEUMATIC artificial muscle (PAM) is a tube-like actuator that largely mimics biological human muscle functions [1]. Compared to traditional electrical motors and hydraulic actuators, the lightweight, high compliance and high power-to-weight ratio of PAMs [2] have fueled their popularity among assistive exoskeletons and rehabilitation robots, such as the upper limb exoskeleton series RUPERT [3] and the lower limb orthotics KAFO [4]. However, unlike the conventional actuators adopted in Lokomat [5] and ArmeoPower [6], the nonlinear and time-varying nature of PAMs may cause difficulties in modeling the robot dynamics [7]. It is thus challenging to maintain high control accuracy of PAMs- driven robots. This work aims to improve the control performance of the PAMs, and the study on single muscle is considered as a prior for actuating the ankle rehabilitation robot [8].

In the past decade, there are amended work on model-based control strategies for PAMs. For instance, Yao et al. proposed a novel empirical model of PAM and designed a self-organizing fuzzy controller with model compensation [9]. Zang et al. developed a modified Prandtl- Ishlinskii model for reproducing the length/pressure hysteresis of PAM, and higher trajectory tracking accuracy has been achieved by a simplex proportional controller with the model-based cascade compensation [10]. In these studies, different mathematical models of PAM and control schemes were established. However, these models are roughly an approximation of the PAM behaviors and tend to miss the dynamic components, so a compensator must be added. In addition, the PAM models include time-varying parameters and nonlinear structures, which will increase the complexity of controller design and analysis. While model-based control schemes have been established, their accuracy and applicability might be limited under different interactive environments or collaboration of multiple PAMs. Therefore, it is imperative to introduce model-free methods for decreasing the PAMs-driven system's sensitivity to dynamic uncertainties in practice [11]. Data-driven model-free control approaches have shown great potential in recent studies [12, 13]. In data-driven schemes, the controller does not have to model the system, instead, only the input and output data will be used [14]. Compared with model-based methods, the data-driven control is more versatile by avoiding the dynamics modelling complexity.

From the recommended rehabilitation strategies, the tasks are often performed in a repetitive manner [15], so the PAM actuators also perform repeated operation modes. This supports the implementation of some form of iterative learning control (ILC), which is well suited for rehabilitation. ILC is a typical data-driven method for controlling repetitively running object, which improves the tracking performance by introducing error data for updating the input of subsequent iterations [16]. However, the unstable function approximation and limited calculation speed of many ILCs make it impractical for PAMs-driven rehabilitation systems [17]. Recently, model-free adaptive control (MFAC) is proposed on the basis of dynamic linearization method, which builds an equivalent data model to replace the original nonlinear model by introducing

Manuscript received January 12, 2019; revised June 11, August 17 and October 3, 2019; accepted October 23, 2019. This work was supported by the National Natural Science Foundation of China under Grant 51675389 and Grant 51705381 and in part by the Key Program for International S&T Cooperation of Hubei Province under Grant 2018AHB007 and the EPSRC Standard Research Scheme under Grant EP/S019219/1. (*Corresponding authors: Wei Meng and Quan Liu*).

Q. Ai, D. Ke, J. Zuo, W. Meng and Q. Liu are with the School of Information Engineering, Wuhan University of Technology, Wuhan 430070 China (e-mails: {weimeng, quanliu}@whut.edu.cn).

W. Meng, Z. Zhang and S. Q. Xie are with the School of Electronic and Electrical Engineering, University of Leeds, Leeds, LS2 9JT, UK. S. Q. Xie is also with College of Electromechanical Engineering, Qingdao University of Science and Technology, Qingdao 266000, China.

the pseudo-partial derivative (PPD) [18]. Different from other data-driven control methods, MFAC is completely model-free, in which the controller parameters can be adaptively adjusted according to the time-varying PPD. A model-free adaptive iterative learning controller (MFAILC) based on iterative dynamic linearization was proposed in [19], where the ILC parameters were updated by previous iteration data. MFAILC has a better suitability to the time-varying systems compared with traditional ILC with fixed gains. Furthermore, the initial condition of MFAILC is not as strict as many ILC methods, which makes it suitable for PAMs-actuated systems.

In repetitive control practice, especially for rehabilitation devices driven by pneumatic muscles, convergence speed is a critical index for iterative learning control [20]. However, current work on improving the convergence is limited [21], so one motivation of this paper is to enhance the convergence performance of MFAILC. In fact, the convergence speed of MFAILC particularly relies on the initial PPD. Without proper selection of initial PPD, it requires multiple attempts to find out the appropriate value [22], which means inappropriate PPD will lead to a slow convergence during the control iterations [23]. In this paper, a high-order pseudo-partial derivative based model-free adaptive iterative learning controller (HOPPD-MFAILC) is proposed which can quickly tune the parameters without large affects from the initial PPD and thus has an enhanced convergence performance.

To our best knowledge, the controller design for PAM based on high-order PPD estimation has not been reported yet. Main contributions of this paper include: 1) By using the high-order PPD estimation scheme based on previous input and output data, the HOPPD-MFAILC method is developed to achieve the high-performance repetitive control of nonlinear time-varying systems such as PAM. Convergence property of the proposed control scheme is independent of the selection of PPDs. However, the existing MFAILC methods will be greatly affected by the initial PPD. 2) This is the first time that a HOPPD-MFAILC is developed for the PAM system with enhanced convergence. The mathematical proof, simulation and experimental results demonstrate that the proposed controller can accelerate the convergence rate compared with existing MFAILC methods. 3) The implementation of HOPPD-MFAILC is completely data-based and model-free, which retains the robustness of closed-loop system in time domain and achieve the convergence of tracking error in iteration domain, even with certain external load interferences. Though the HOPPD-MFAILC is developed under the consideration of PAM, it is also applicable to other nonlinear systems.

The rest of this paper is organized as follows. Section II introduces the problem formulation and the HOPPD-MFAILC controller design then the enhanced convergence is analyzed theoretically. Some simulation and PAM control experiments for validation and comparison are demonstrated in Section III and discussion and conclusion are given in Section IV.

II. CONTROL STRATEGY

A. Model-Free Adaptive Iterative Learning Control

MFAILC is a completely model-free method. Basically, the method aims to establish a dynamic linearization (DL) model of the system between any two adjacent iterations, and then to derive the controller structure and parameter using the model. Three commonly used DL models include compact-form DL (CFDL), partial-form DL (PFDL) and full-form DL (FFDL) [24]. The proposed method is based on CFDL model.

Considering the following repeatable nonlinear discrete-time SISO (single input, single output) system:

$$\begin{aligned} y_k(t+1) = f(&y_k(t), y_k(t-1), \cdots, y_k(t-n_y), \\ &u_k(t), u_k(t-1), \cdots, u_k(t-n_u)) \end{aligned} \tag{1}$$

where $u_k(t)$ and $y_k(t)$ denote the control input and output of the system at time t of the *k-th* iteration. $t=0,1,2\cdots,T-1$, and T is the endpoint of the finite time interval. n_y and n_u are two unknown positive integers representing the system order. $f(\cdot)$ is an unknown nonlinear function. For system (1), the aim of this controller is to find out a suitable sequence of bounded control input $u_k(t)$ such that the system output sequence $y_k(t)$ is able to track the given desired trajectory $y_d(t)$.

The following assumptions for system (1) are given to make the discussion rigorous [19].

Assumption 1: The partial derivative of the nonlinear function $f(\cdot)$ with respect to the input $u_k(t)$ is continuous.

Assumption 2: System (1) is generalized Lipschitz, that is, for all $t=0,1,2\cdots,T-1$ and $k=0,1,2\cdots$, if $\left|\Delta u_k(t)\right| \neq 0$, then the system (1) satisfies the following condition:

$$\left|\Delta y_k(t+1)\right| \le b\left|\Delta u_k(t)\right| \tag{2}$$

where $\Delta y_k(t+1) = y_k(t+1) - y_{k-1}(t+1)$, $\Delta u_k(t) = u_k(t) - u_{k-1}(t)$, and b is a positive constant.

Assumption 1 is typical in general nonlinear system control. Assumption 2 gives the relationship between the incremental input and the incremental output along the iterative axis at any time. The constant b is determined by trials for qualitative analysis, which means a finite input change will result in a finite output change and it is reasonable for general systems.

Based on the above two assumptions, the following Lemma [19] can be achieved:

Lemma 1: Considering system (1) satisfies Assumption 1&2, for all $\Delta u_k(t) \neq 0$, there exists a function $\phi_k(t)$ such that the system can be converted into the following CFDL data:

$$\Delta y_k(t+1) = \phi_k(t)\Delta u_k(t) \tag{3}$$

where $\phi_k(t)$ is called pseudo-partial derivative which satisfies $|\phi_k(t)| \le b$. The detailed proof can be found in [19].

Define the following criteria function:

$$J(u_k(t)) = \left|y_d(t+1) - y_k(t+1)\right|^2 + \lambda\left|u_k(t) - u_{k-1}(t)\right|^2 \tag{4}$$

where λ is a weighting coefficient. Substituting (3) into the criterion function (4), we can get:

$$J(u_k(t)) = \left|e_{k-1}(t+1) - \phi_k(t)(u_k(t) - u_{k-1}(t))\right|^2 + \lambda\left|u_k(t) - u_{k-1}(t)\right|^2 \tag{5}$$

Then we have the derivation of (5) as below:

$$\begin{aligned} \frac{\partial J(u_k(t))}{\partial u_k(t)} =& 2(-\phi_k(t))(e_{k-1}(t+1) - \phi_k(t)(u_k(t) - u_{k-1}(t))) \\ &+ 2\lambda(u_k(t) - u_{k-1}(t)) \end{aligned} \tag{6}$$

To get the optimal solution for minimizing (5) [20, 25] with respect to $u_k(t)$, we solve $\partial J(u_k(t)) / \partial u_k(t) = 0$, gives:

$$\phi_k(t)e_{k-1}(t+1) = \left|\phi_k(t)\right|^2((u_k(t) - u_{k-1}(t)) + \lambda(u_k(t) - u_{k-1}(t)) \tag{7}$$

$$\left(\lambda+\left|\phi_k(t)\right|^2\right)(u_k(t)-u_{k-1}(t))=\phi_k(t)e_{k-1}(t+1) \tag{8}$$

$$u_k(t)-u_{k-1}(t)=\frac{\phi_k(t)e_{k-1}(t+1)}{\lambda+\left|\phi_k(t)\right|^2} \tag{9}$$

Thus, $u_k(t)$ can be expressed by (10):

$$u_k(t)=u_{k-1}(t)+\frac{\rho_{k,t}\phi_k(t)}{\lambda+\left|\phi_k(t)\right|^2}e_{k-1}(t+1) \tag{10}$$

where $\rho_{k,t}$ is a step factor designed to make the controller be more universal [21], and $e_{k-1}(t+1)=y_d(t+1)-y_{k-1}(t+1)$ is the tracking error. Since $\phi_k(t)$ is unknown, the following criteria function with the estimated parameter is defined:

$$J(\hat{\phi}_k(t))=\left|\Delta y_{k-1}(t+1)-\hat{\phi}_k(t)\Delta u_{k-1}(t)\right|^2+\mu\left|\hat{\phi}_k(t)-\hat{\phi}_{k-1}(t)\right|^2 \tag{11}$$

where μ is the weighting coefficient and $\hat{\phi}_k(t)$ is the estimated value of $\phi_k(t)$. Eq. (11) indicates that the target constrained input should be as small as possible while the tracking error is minimized, which means $\hat{\phi}_k(t)$ will converge to $\phi_k(t)$.

Based on the derivation of (11) as below and $\partial J(\hat{\phi}_k(t))/\partial\hat{\phi}_k(t)=0$, the estimation algorithm is expressed by (12):

$$\frac{\partial J(\hat{\phi}_k(t))}{\hat{\phi}_k(t)}=2(\Delta u_{k-1}(t))(\Delta y_{k-1}(t+1)-\hat{\phi}_k(t)\Delta u_{k-1}(t))+2\mu(\hat{\phi}_k(t)-\hat{\phi}_{k-1}(t))$$

$$\hat{\phi}_k(t)=\hat{\phi}_{k-1}(t)+\frac{\eta_{k,t}\Delta u_{k-1}(t)}{\mu+\left|\Delta u_{k-1}(t)\right|^2}(\Delta y_{k-1}(t+1)-\hat{\phi}_{k-1}(t)\Delta u_{k-1}(t)) \tag{12}$$

where $\eta_{k,t}$ is the step factor.

To ensure that the iterative dynamic linearization model is always true, and to make compensation to the time-varying parameter, the following reset algorithm is applied:

$$\hat{\phi}_k(t)=\hat{\phi}_0(t),\ \text{if}\ \hat{\phi}_k(t)\le\varepsilon\ \text{or}\ \left|\Delta u_k(t)\right|\le\varepsilon \tag{13}$$

where ε is a positive constant, and $\hat{\phi}_0(t)$ is the initial value of $\hat{\phi}_k(t)$. So, the MFAILC-based CFDL data model is constructed by the iterative learning law (10), the estimation algorithm (12), and the reset algorithm (13). It is a data-driven method that only utilizes the input and output data of the system. Compared with traditional ILCs, the gain parameter composed of $\hat{\phi}_k(t)$ is not fixed, instead, it will be updated iteratively.

B. High-Order PPD Estimation Algorithm

The estimation algorithm (12) in original MFAILC scheme runs along the iterative axis, which can be regarded as a kind of parameter tuning law. Differently in our method, to achieve a faster convergence, a high-order iterative learning law (14) is designed based on previous iterations [25].

$$u_k(t)=\sum_{i=1}^{l_u}a_iu_{k-i}(t)+\sum_{j=1}^{l_e}b_je_{k-j}(t+1) \tag{14}$$

where l_u and l_e are integers as the order, a_i, b_j the weighting coefficient of the input and error terms, with $\sum_{i=1}^{l_u}a_i=1$, $\sum_{j=1}^{l_e}b_j=1$.

In criterion function (11), $\Delta y_{k-1}(t+1)-\hat{\phi}_k(t)\Delta u_{k-1}(t)$ represents the model error of the iterative dynamic linearization model (3) in which $\phi_k(t)$ is replaced by $\hat{\phi}_k(t)$ as the input. A high-order parameter estimation algorithm for PPD is proposed here by updating the criterion function (11) as follows:

$$\begin{aligned}J(\hat{\phi}_k(t))&=\left|\Delta y_{k-1}(t+1)-\hat{\phi}_k(t)\Delta u_{k-1}(t)\right|^2\\&+\mu\left|\hat{\phi}_k(t)-\sum_{i=1}^{m}\alpha_i\hat{\phi}_{k-i}(t)\right|^2\end{aligned} \tag{15}$$

where m is the order, α_i is weighting coefficient with $\sum_{i=1}^{m}\alpha_i=1$.

So the high-order estimation algorithm is expressed by (16) based on the derivation of (15) below and $\partial J(\hat{\phi}_k(t))/\partial\hat{\phi}_k(t)=0$:

$$\frac{\partial J(\hat{\phi}_k(t))}{\hat{\phi}_k(t)}=2(-\hat{\phi}_k(t))(\Delta y_{k-1}(t+1)-\hat{\phi}_k(t)\Delta u_{k-1}(t))+2\mu(\hat{\phi}_k(t)-\sum_{i=1}^{m}\alpha_i\hat{\phi}_{k-i}(t))$$

$$\hat{\phi}_k(t)=\frac{\Delta u_{k-1}(t)\Delta y_{k-1}(t+1)}{\mu+\left|\Delta u_{k-1}(t)\right|^2}+\frac{\mu\eta_{k,t}}{\mu+\left|\Delta u_{k-1}(t)\right|^2}\sum_{i=1}^{m}\alpha_i\hat{\phi}_{k-i}(t) \tag{16}$$

The forms of iterative learning law and the reset algorithm remain the same as MFAILC, with the PPD being estimated by the high-order algorithm. Therefore, the overall control scheme of the proposed HOPPD-MFAILC is described as (17)-(19), and the controller diagram is illustrated in Fig. 1.

$$\begin{cases}\hat{\phi}_k(t)=\hat{\phi}_{k-1}(t)+\dfrac{\eta_{k,t}\Delta u_{k-1}(t)}{\mu+\left|\Delta u_{k-1}(t)\right|^2}\\ \quad\times(\Delta y_{k-1}(t+1)-\hat{\phi}_{k-1}(t)\Delta u_{k-1}(t)) & 2\le k<m\\ \hat{\phi}_k(t)=\dfrac{\Delta u_{k-1}(t)\Delta y_{k-1}(t+1)}{\mu+\left|\Delta u_{k-1}(t)\right|^2}\\ \quad+\dfrac{\mu\eta_{k,t}}{\mu+\left|\Delta u_{k-1}(t)\right|^2}\sum_{i=1}^{m}\alpha_i\hat{\phi}_{k-i}(t) & k\ge m\end{cases} \tag{17}$$

$$\hat{\phi}_k(t)=\hat{\phi}_0(t),\ \text{if}\ \hat{\phi}_k(t)\le\varepsilon\ \text{or}\ \left|\Delta u_k(t)\right|\le\varepsilon \tag{18}$$

$$u_k(t)=u_{k-1}(t)+\frac{\rho_{k,t}\hat{\phi}_k(t)}{\lambda+\left|\hat{\phi}_k(t)\right|^2}e_{k-1}(t+1) \tag{19}$$

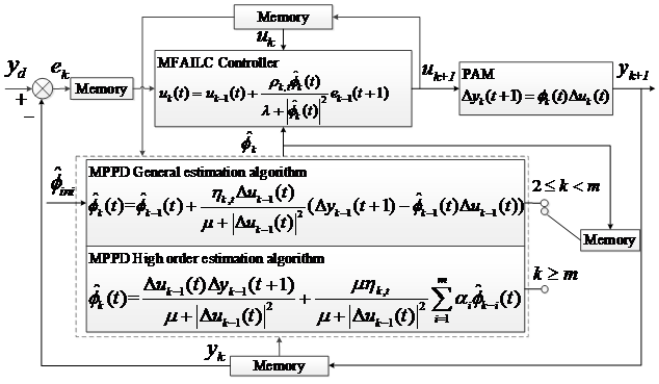

Fig. 1. Block diagram of the proposed HOPPD-MFAILC.

Remark 1: Different from those high-order algorithms using control input [26] and tracking error terms [27] from previous iterations to improve the learning control law, the high-order estimation algorithm applied here as in (16) contributes to improvement of the controller parameters themselves.

Remark 2: In the first two iterations, initial values need to be assigned to $\hat{\phi}_0(t)$ and $\hat{\phi}_1(t)$. Since $\hat{\phi}_k(t)$ is calculated based on the previous m iterations, it can only be obtained when $k\ge m$, so the high-order estimation algorithm (16) is applied under $k\ge m$. However, when $2\le k<m$, i.e., no previous iterations are available, the original estimation algorithm (12) is used.

Remark 3: The usage of weighting coefficients α_i in the high-order estimation algorithm (16) is similar to the forgetting

factor in the general ILC schemes. Therefore, they can be set as $\alpha_1 \geq \alpha_2 \geq \cdots \geq \alpha_m$.

C. Convergence Analysis

Assumption 3: For all $k \in \{0,1,2\cdots\}$ and $t \in \{0,1,2,\cdots,T-1\}$, $\phi_k(t)$ satisfies $\phi_k(t) \geq 0$ (or $\phi_k(t) \leq 0$), and $\phi_k(t)=0$ is only established at a finite point.

Assumption 3 is inspired by [19]. In our system, with the increase of air input, PAM will contract and the displacement will increase. Such change of displacement and control input satisfies the positive correlation described in Assumption 3. Then the following theorem can be obtained:

Theorem 1: For system (1), if Assumption 3 holds, the HOPPD-MFAILC scheme has the following properties:

i) for $k \in \{0,1,2\cdots\}$ and $t \in \{0,1,2,\cdots,T-1\}$, $\hat{\phi}_k(t)$ is bounded;

ii) when $k \to \infty$, the tracking error converges to zero;

iii) for $k \in \{0,1,2\cdots\}$ and $t \in \{0,1,2,\cdots,T-1\}$, $u_k(t)$ is bounded.

Proof

When $\hat{\phi}_k(t) \leq \varepsilon$ or $|\Delta u_k(t)| \leq \varepsilon$, $\hat{\phi}_k(t)=\hat{\phi}_0(t)$, $\hat{\phi}_0(t)$ is bounded.

In other case, when $2 \leq k < m$, subtract $\phi_k(t)$ from both sides of (17), and let $\tilde{\phi}_k(t)=\hat{\phi}_k(t)-\phi_k(t)$, we have:

$$\begin{aligned}\tilde{\phi}_k(t)&=\tilde{\phi}_{k-1}(t)-(\phi_k(t)-\phi_{k-1}(t))\\&+\frac{\eta_{k,t}\Delta u_{k-1}(t)}{\mu+|\Delta u_{k-1}(t)|^2}(\Delta y_{k-1}(t+1)-\hat{\phi}_{k-1}(t)\Delta u_{k-1}(t))\end{aligned} \tag{20}$$

Let $\Delta\phi_k(t)=\phi_k(t)-\phi_{k-1}(t)$, substituting (3) into (20), and take the absolute value at both sides, we have:

$$\begin{aligned}|\tilde{\phi}_k(t)| &\leq \varphi_1|\tilde{\phi}_{k-1}(t)|+2b \leq \varphi_1^2|\tilde{\phi}_{k-2}(t)|+(1+\varphi_1)2b\\&\leq \cdots \leq \varphi_1^m|\tilde{\phi}_0(t)|+\frac{1-\varphi_1^{m-1}}{1-\varphi_1}2b\end{aligned} \tag{21}$$

where $\varphi_1=\sup_{k\in\{0,1,\cdots,m-1\}}\sup_{t\in\{0,1,\cdots,T\}}\left\{\left|1-\frac{\eta_{k,t}\Delta u^2{}_{k-1}(t)}{\mu+|\Delta u_{k-1}(t)|^2}\right|\right\}$.

Since m is a bounded order which is manually set during the control process, $\tilde{\phi}_k(t)$ is bounded as long as $0<\varphi_1<1$. Since $|\Delta u_k(t)| \neq 0$, there exist suitable $\eta_{k,t}$ and μ such that $0<\varphi_1<1$. So, we get $\tilde{\phi}_k(t)$ is bounded. According to Lemma 1, we have that $\phi_k(t)$ is bounded, and that $\hat{\phi}_k(t)$ is also bounded.

When $|\Delta u_k(t)| > \varepsilon$ and $k \geq m$, we have from (17) that:

$$\hat{\phi}_k(t)=\frac{\Delta u_{k-1}(t)\Delta y_{k-1}(t+1)}{\mu+|\Delta u_{k-1}(t)|^2}+\frac{\mu\eta_{k,t}}{\mu+|\Delta u_{k-1}(t)|^2}\sum_{i=1}^{m}\alpha_i\hat{\phi}_{k-i}(t)$$

Substituting (3) into equation above and taking the absolute value at both sides, we can have (22).

$$\begin{aligned}|\hat{\phi}_k(t)|&=\left|\frac{\phi_{k-1}(t)\Delta u_{k-1}^2(t)}{\mu+|\Delta u_{k-1}(t)|^2}+\frac{\mu\eta_{k,t}}{\mu+|\Delta u_{k-1}(t)|^2}\sum_{i=1}^{m}\alpha_i\hat{\phi}_{k-i}(t)\right|\\&\leq|\phi_{k-1}(t)|\left|1-\frac{\mu}{\mu+|\Delta u_{k-1}(t)|^2}\right|+|\eta_{k,t}|\sum_{i=1}^{m}|\alpha_i\hat{\phi}_{k-i}(t)|\left|1-\frac{|\Delta u_{k-1}(t)|^2}{\mu+|\Delta u_{k-1}(t)|^2}\right|\\&<|\phi_{k-1}(t)|+|\eta_{k,t}|\sum_{i=1}^{m}|\alpha_i\hat{\phi}_{k-i}(t)|\\&<\cdots<|\phi_{k-1}(t)|+|\eta_{k,t}|\sum_{j=1}^{k-m+1}\sum_{i=1}^{m}|\alpha_i\hat{\phi}_{k-i}(t)|\end{aligned} \tag{22}$$

According to Lemma 1, we can get that $\phi_k(t)$ is bounded, so $|\phi_{m-1}(t)|$ is bounded. Since the boundedness of $\hat{\phi}_{k-1}$ when $2 \leq k < m$ has been proved, $|\eta_{k,t}|\sum_{j=1}^{k-m+1}\sum_{i=1}^{m}|\alpha_i\hat{\phi}_{k-i}(t)|$ is bounded. Therefore, $\hat{\phi}_k(t)$ is bounded. Then we prove the convergence of tracking error and the boundedness of control input as follows.

According to Lemma 1 and (19), we have:

$$\begin{aligned}e_k(t+1)&=y_d(t+1)-y_{k-1}(t+1)-\phi_k(t)\Delta u_k(t)\\&=(1-\phi_k(t)\frac{\rho_{k,t}\hat{\phi}_k(t)}{\lambda+|\hat{\phi}_k(t)|^2})e_{k-1}(t+1)\end{aligned} \tag{23}$$

In traditional model-free adaptive iterative learning control schemes, the PPD estimation algorithm (12) operates along the iteration axis, which can be regarded as a kind of parameter tuning law. The general learning law is basically composed of control input and tracking error terms, while using high-order method, the form of learning law can be written as below.

$$u_k(t)=u_{k-1}(t)+\frac{\rho_{k,t}\hat{\phi}_k(t)}{\lambda+|\hat{\phi}_k(t)|^2}e_{k-1}(t+1)$$

Compared with traditional control schemes, the proposed higher-order iterative learning law can make use of the data in previous iterations and would achieve faster error convergence [28]. Taking norms on both sides of (23), yields:

$$\begin{aligned}|e_k(t+1)|&=\left|1-\phi_k(t)\frac{\rho_{k,t}\hat{\phi}_k(t)}{\lambda+|\hat{\phi}_k(t)|^2}\right||e_{k-1}(t+1)|\\&\leq d_2|e_{k-1}(t+1)| \leq \cdots \leq d_2^k|e_0(t+1)|\end{aligned} \tag{24}$$

where $d_2=\sup_{k\in\{0,1,\cdots,\infty\}}\sup_{t\in\{0,1,\cdots,T-1\}}\left\{\left|1-\frac{\rho_{k,t}\phi_k(t)\hat{\phi}_k(t)}{\lambda+|\hat{\phi}_k(t)|^2}\right|\right\}$.

Obviously, if $0<d_2<1$, it can guarantee that the tracking error $e_k(t+1)$ converges to zero when $k \to \infty$.

Since $\phi_k(t)$ and $\hat{\phi}_k(t)$ are both bounded, from Assumption 3, (17) and (18), we can get $\phi_k(t)\hat{\phi}_k(t)>0$.

Solving the inequality equation $\left|1-\frac{\rho_{k,t}\phi_k(t)\hat{\phi}_k(t)}{\lambda+|\hat{\phi}_k(t)|^2}\right|<1$, gives:

$$0<\rho_{k,t}<\frac{2(\lambda+\hat{\phi}_k(t)^2)}{\phi_k(t)\hat{\phi}_k(t)} \tag{25}$$

From above analysis, $\phi_k(t)$ and $\hat{\phi}_k(t)$ are bounded and $\hat{\phi}_k(t)$ converges to $\phi_k(t)$. The boundary of $\phi_k(t)$ is $|\phi_k(t)| \leq b$. We know $\lambda>0$, it gets $2(\lambda+\hat{\phi}_k(t)^2)/\phi_k(t)\hat{\phi}_k(t)>2\hat{\phi}_k(t)^2/\phi_k(t)\hat{\phi}_k(t)$, which equals to 2 within iterations. Selecting appropriate λ and $\rho_{k,t}$, e.g., $0<\rho_{k,t}<2$, to satisfy (25) guarantees that for all $k \in \{0,1,2\cdots\}$ and $t \in \{0,1,2,\cdots,T-1\}$, $0<d_2<1$ always holds. Such that, the inequality (24) also follows and the stability of the closed loop system can be guaranteed.

Consequently, the tracking error will converge to zero.

According to (19), we have:

$$\Delta u_k(t)=\frac{\rho_{k,t}\hat{\phi}_k(t)}{\lambda+|\hat{\phi}_k(t)|^2}e_{k-1}(t+1) \tag{26}$$

As $\hat{\phi}_k(t)$ is bounded, there must exist a constant N

$$N = \sup_{k\in[0,\infty)} \sup_{t\in\{0,1,\cdots,T-1\}} \left\{ \frac{\rho_{k,t}\hat{\phi}_k(t)}{\lambda + \left|\hat{\phi}_k(t)\right|^2} \right\}$$

such that

$$\left|\Delta u_k(t)\right| \le N \left|e_{k-1}(t+1)\right| \tag{27}$$

Since

$$\begin{aligned} \left|u_k(t)\right| &= \left|u_k(t) - u_0(t) + u_0(t)\right| \le \left|u_k(t) - u_0(t)\right| + \left|u_0(t)\right| \\ &= \left|u_k(t) - u_{k-1}(t) + u_{k-1}(t) - \cdots + u_1(t) - u_0(t)\right| + \left|u_0(t)\right| \\ &\le \left|\Delta u_k(t)\right| + \left|\Delta u_{k-1}(t)\right| + \cdots + \left|\Delta u_1(t)\right| + \left|u_0(t)\right| \end{aligned} \tag{28}$$

According to (23), (27) and (28), we have:

$$\begin{aligned} \left|u_k(t)\right| &\le N\left|e_{k-1}(t+1)\right| + N\left|e_{k-2}(t+1)\right| + \cdots \\ &\quad + N\left|e_0(t+1)\right| + \left|u_0(t)\right| \\ &\le N\frac{d_2}{1-d_2}\left|e_0(t+1)\right| + \left|u_0(t)\right| \end{aligned} \tag{29}$$

Both $u_0(t)$ and $e_0(t+1)$ can be set initially bounded, from (29) it follows that for all $k \in \{0,1,2\cdots\}$ and $t \in \{0,1,2,\cdots,T-1\}$, $u_k(t)$ is bounded. Thus (16) is the high-order estimation of pseudo-partial derivatives and $\eta_{k,t}$ is the step size factor.

For control scheme (17), the term $\Delta y_{k-1}(t+1) - \hat{\phi}_k(t)\Delta u_{k-1}(t)$ represents the estimation error of the dynamic linearization model (3) when PPD estimation is adopted, and $\hat{\phi}_k(t)$ is equivalent to the model input. Therefore, (15) can be regarded as a criterion function similar to (4). Higher order form of input and estimation can improve the estimation speed of PPDs and this has been proved with faster convergence [26]. From (24) we obtain the exponential convergence of the output error in iteration domain with a faster convergence speed. Furthermore, the high-order estimation algorithm makes use of the PPDs in the previous *m* iterations, so the current PPD can learn more from the past data, thus achieving enhanced convergence. This will also be verified by the simulation and experiments.

III. Simulation and Experiments

A. Simulation Validation

To verify effectiveness of the proposed HOPPD-MFAILC, simulation experiments are conducted on a time-varying model, followed by the control on actual PAM. The system (30) contains time-varying parameters and repetitive interferences [19], which can reflect the PAM's nonlinear features and is thus introduced as the controlled object.

$$y(t+1) = \begin{cases} \dfrac{y(t)}{1+y^2(t)} + u^3(t), & 0 \le t \le 50 \\ (y(t)y(t-1)y(t-2)u(t-1) & \\ \times(y(t-2)-1) + \alpha(t)u(t)) & \\ /(1+y^2(t-1)+y^2(t-2)), & 50 < t \le 100 \end{cases} \tag{30}$$

where $\alpha(t) = 0.1 * round(t/50)$ is the time-varying parameter of the system. Define the desired trajectory as:

$$y_d(t+1) = \begin{cases} 0.5*(-1)^{round(t/10)}, & 0 \le t \le 30 \\ 0.5*\sin(t\pi/10) & \\ +0.3*\cos(t\pi/10), & 30 < t \le 70 \\ 0.5*(-1)^{round(t/10)}, & 70 < t \le 100 \end{cases} \tag{31}$$

Both MFAILC and HOPPD-MFAILC are used to control the system (30) in simulation tests. For MFAILC, the controller parameters are λ=0.6, $\rho_{k,t}$=1, μ=0.1 and $\eta_{k,t}$=0.6. For HOPPD-MFAILC, the order of high-order estimation is set to $m=3$, the weighting coefficients are $\alpha_1 = 0.4$, $\alpha_2 = 0.4$, $\alpha_3 = 0.2$, and the high-order estimation algorithm starts from the 4th iteration. The initial PPD is set as $\hat{\phi}_0$=10 for both controllers.

Fig. 2 shows the tracking results of the MFAILC and the HOPPD-MFAILC, where the red solid line denotes the desired trajectory and the dotted lines denote the actual trajectories in different iterations. Results from the 2nd, 3rd, 4th iteration to the 20th, 40th iteration indicate that the actual trajectory can gradually approach the desired one and completely track it in a finite number of iterations. HOPPD-MFAILC possesses a better trajectory tracking performance than MFAILC within 20 and 40 iterations. Though the object cannot be controlled with good performance in the first several iterations due to the lack of initial operations, it can still converge to the desired trajectory within several iterations. The tracking errors in the first several iterations are within a controllable range [21], which will not happen in real-life testing, as the first two operations will be predefined in actual experiments [17]. This can also be proved by the following PAM experiments.

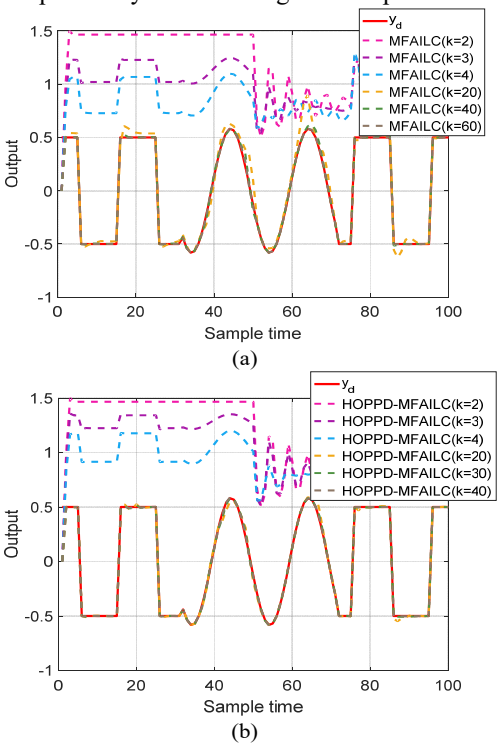

Fig. 2. Trajectory tracking results of the model in simulation controlled by (a) MFAILC and (b) HOPPD-MFAILC with $\hat{\phi}_0$ =10 .

Since the initial PPD will have a great influence on the convergence speed of the algorithm, comparative experiments of different initial PPDs are conducted. We set the same initial

value for HOPPD-MFAILC and MFAILC to compare their performance starting from the same condition. The maximum error convergence curves of MFAILC and HOPPD-MFAILC with different initial PPDs are shown in Fig. 3. We can see that the change of initial PPD has greatly affected the convergence speed of MFAILC method, while HOPPD-MFAILC scheme demonstrates a better control performance and high robustness. HOPPD-MFAILC is able to improve the convergence speed of the maximum tracking error, and the less appropriate the initial PPD is, the more obvious improvement of the convergence performance can be seen. Results show that HOPPD-MFAILC scheme can always achieve a faster convergence speed whether the initial PPD is properly selected or not.

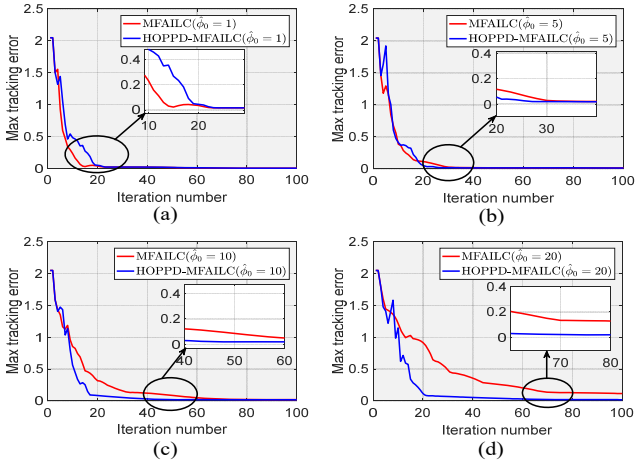

Fig. 3. Comparison of maximum tracking error convergence between MAFILC and HOPPD-MFAILC with different initial PPDs. (a), (b), (c), (d) represent the convergence curves with $\hat{\phi}_0 = 1, 5, 10, 20$, respectively.

To further investigate the effect of PPDs, Fig. 4 shows the variation of PPD along the time axis and that along the iterative axis with $\hat{\phi}_0 = 10$ for MFAILC and HOPPD-MFAILC. From the change of $\hat{\phi}(k,t)$ along the iterative axis at each sample time, we confirm that the HOPPD-MFAILC can converge with less iterations than MFAILC. Meanwhile, it can be seen that the HOPPD-MFAILC scheme converges to the same value as MFAILC, which means that HOPPD-MFAILC can improve the convergence speed of MFAILC but still maintain the control capacity of MFAILC to achieve the similar accuracy.

Meanwhile, the high-order estimation algorithm starts from which iteration also has an influence on the convergence. Fig. 5 shows the comparison of error convergence results when using HOPPD-MFAILC starting from different iterations, and k_0 is the start iteration. It can be seen that the earlier high-order parameter estimation algorithm is used along the iterative axis, the faster the tracking error converges. It also indicates that the proposed HOPPD-MFAILC is indeed superior to the MFAILC method in terms of convergence performance.

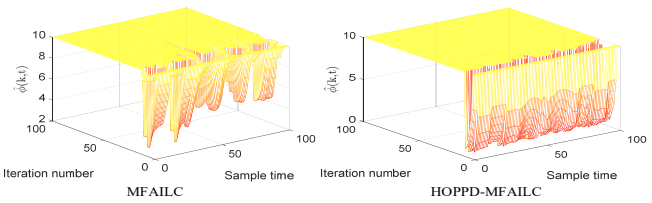

Fig. 4. Variation of PPD $\hat{\phi}(k,t)$ in MFACILC and HOPPD-MFAILC.

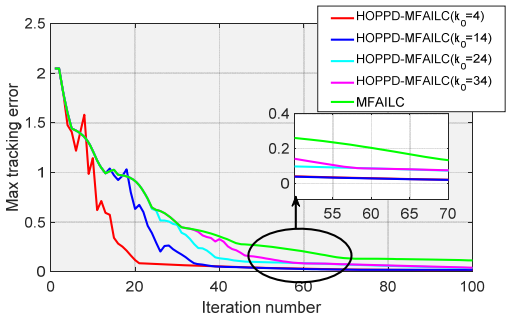

Fig. 5. Maximum tracking error convergence of HOPPD-MFAILC when start using high-order estimation algorithm from different iterations.

B. PAM Control Experiments

To verify the performance of HOPPD-MFAILC in practical nonlinear and dynamic system control, we developed a PAM control testing platform, as shown in Fig. 6. One end of the PAM (FESTO MAS-20-400N) is suspended on a rigid frame and the other end is free-moving. The control system is implemented on LabVIEW. The resulted controller output is sent to the proportional valve (VPPM-6L-G18-0L6H) through NI roboRIO. The valve regulates the air pressure inside the PAM to realize trajectory tracking control. Displacement of the PAM is measured by a position sensor (MLO POT-225-TLF) linked with the muscle free-moving end and will be feedback to the control program in real time via NI roboRIO.

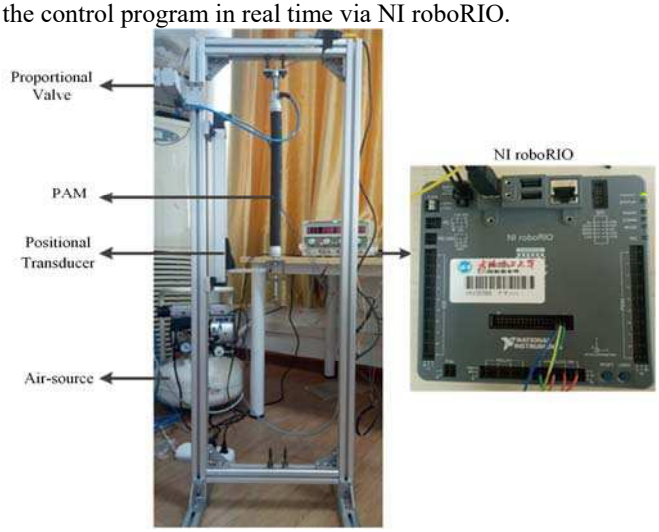

Fig. 6. Experiment setup for controller tests on PAM.

The desired trajectory of PAM is set to $y_d = 2.3 + 2\sin(\pi t)$. For comparison study, both MFAILC and HOPPD-MFAILC schemes are used to control the PAM system successively. The controller parameters of MFAILC are set as λ=1, $\rho_{k,t}$=5, μ=1 and $\eta_{k,t}$=0.6. For HOPPD-MFAILC, the order of the estimation algorithm is set to $m = 3$, weighting coefficients are $\alpha_1 = 0.5$, $\alpha_2 = 0.3$, $\alpha_3 = 0.2$, and the iteration that the high-order estimation algorithm starts is set to 4. The initial PPD for both schemes is $\hat{\phi}_0 = 40$, with all other parameters unchanged.

The tracking results of both methods are shown in Fig. 7, where the red solid line denotes the desired trajectory, and the dotted lines denote the actual trajectories in different iterations. It indicates that the actual trajectory of PAM is able to gradually follow the desired trajectory with iterations. The final trajectory

tracking error is maintained under 2mm, which is acceptable in practice due to some inevitable measurement errors or external disturbances. Compared with the results of MFAILC in Fig. 7(a), it can be obviously seen from Fig. 7(b) that the proposed HOPPD-MFAILC method can track the desired trajectory more efficiently, for example, it can reach a satisfactory accuracy within 9 iterations, while the MFAILC method cannot achieve this level until the 15th iteration.

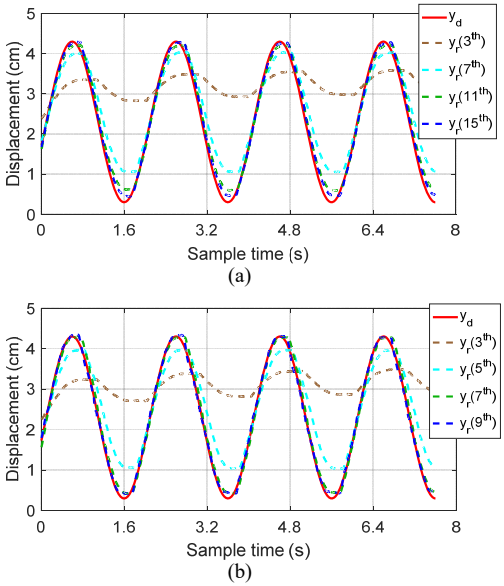

Fig. 7. Trajectory tracking results of the PAM in practice controlled by (a) MFAILC and (b) HOPPD-MFAILC with $\hat{\phi}_0 = 40$.

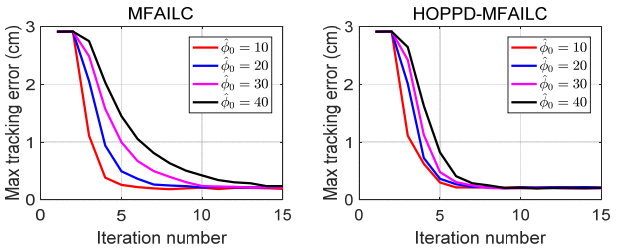

Fig. 8. Convergence curves of maximum tracking error in MFAILC and HOPPD-MFAILC with different initial PPDs when controlling a PAM.

The convergence curves of the maximum tracking errors of MFAILC and HOPPD-MFAILC with different initial PPDs are shown in Fig. 8. We can conclude similarly with the simulation test that the initial PPD affects the convergence speed. In case of $\hat{\phi}_0 = 10$, MFAILC method can achieve a fast convergence of the maximum tracking error, and HOPPD-MFAILC method maintains a similar performance. With the variation of PPD from 20 to 30 and 40, HOPPD- MFAILC method demonstrates more tracking improvements and better superior convergence performance over MFAILC. Specifically, HOPPD-MFAILC method can reduce the time cost of about 2, 5 and 8 iterations when $\hat{\phi}_0 = 20$, $\hat{\phi}_0 = 30$ and $\hat{\phi}_0 = 40$, respectively.

To further validate the proposed controller's performance, the comparison of results under three different frequencies (0.5Hz, 2.5 Hz and 5Hz) and $\hat{\phi}_0 = 40$ while other parameters unchanged is shown in Fig. 9, where the resulted trajectories and the maximum error convergence curves at different frequencies are presented. Except for some error differences in the first several iterations, the maximum tracking errors can converge to a low value quickly. The control performance of the proposed method does not change much over frequencies and is still satisfactory even at higher frequencies.

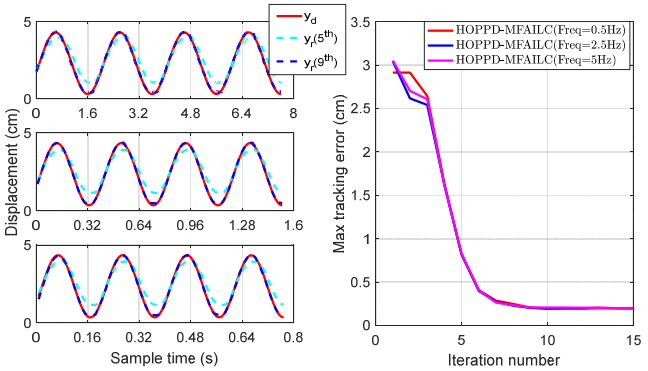

Fig. 9. Tracking results and maximum error convergence of PAM controlled by HOPPD-MFAILC at different frequencies ($\hat{\phi}_0 = 40$).

To illustrate the effect of high-order estimation algorithm on the convergence speed, a longitudinal comparison experiment is performed under condition that other controller parameters unchanged. The comparison study is to apply the high-order estimation algorithm to PPD starting from different iterations. Fig. 10 illustrates the convergence curves of the maximum tracking error starting from the 4th, the 8th, and the 12th iteration. It is clear that once applying the high-order estimation algorithm to PPD, the convergence performance will be greatly enhanced immediately, which means the HOPPD-MFAILC scheme is able to increase the convergence speed. This conclusion is also in consistent with the simulation.

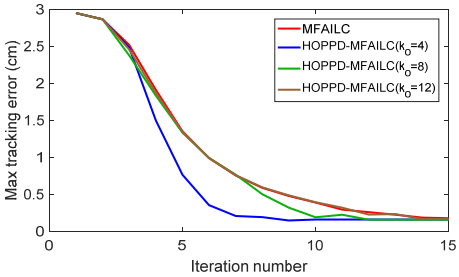

Fig. 10. Maximum tracking error convergence of PAM controlled by HOPPD-MFAILC using high-order estimation from different iterations.

Robustness performance of the HOPPD-MFAILC is also investigated, as the PAMs-driven rehabilitation robot will be finally controlled with human interactions. Compared with non-load operation of the robot, the load of the affected limb during rehabilitation will inevitably cause interferences to the robot, and the tracking accuracy will be affected. In order to verify the controller's capacity in disturbance tolerance, two types of load interferences are added to the PAM: the load along the time axis ($d = 0.5 + 0.5\sin(\pi t)$) and the random load interference along the iteration axis, as shown in Fig. 11. The tracking results of HOPPD-MFAILC are shown in Fig. 12, where (a) is the tracking results after adding load interference along the time axis, and (b) is the tracking results after adding load interference along the iteration axis. All other control parameters maintain consistent with the HOPPD-MFAILC above. Comparing Fig. 12 with Fig. 7(b), there is no significant difference on the tracking results between the two cases, which

indicates the HOPPD-MFAILC's good robustness and superior capacity in handling external load interferences and these make it suitable for human robot interactive applications.

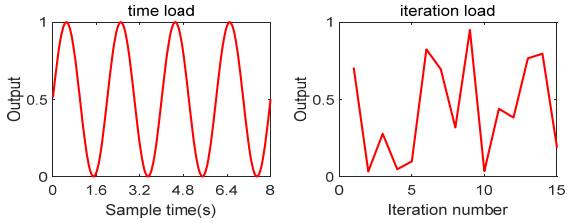

Fig. 11. The sine wave load interference added to PAM along the time axis and the random load interference along the iteration axis.

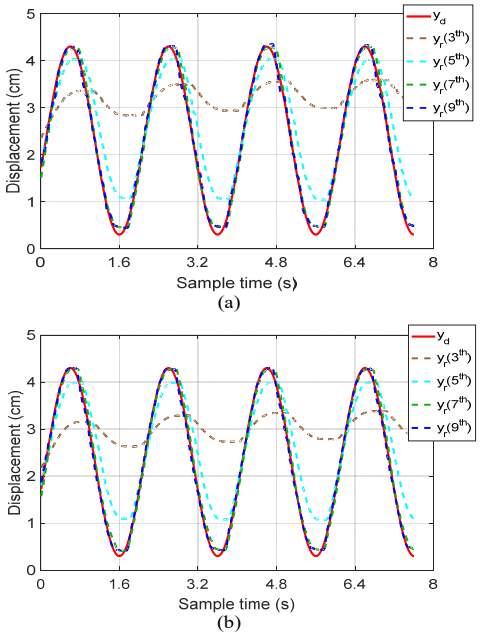

Fig. 12. Tracking results of PAM controlled by HOPPD-MFAILC with load interferences along (a) the time axis and (b) the iteration axis.

Fig. 13 further presents the comparison of the convergence performance of HOPPD-MFAILC with and without load interference in PAM control when $\hat{\phi}_0 = 30$. The left shows the comparison of maximum tracking error between PAM controls with and without load interference along time axis, and the right shows the comparison between controls with and without load interference along iteration axis. From Fig. 13, we can conclude that the HOPPD-MFAILC's convergence performance will not be greatly influenced by the load interferences, which means the HOPPD-MFAILC still maintains a superior convergence performance even with certain random load interferences.

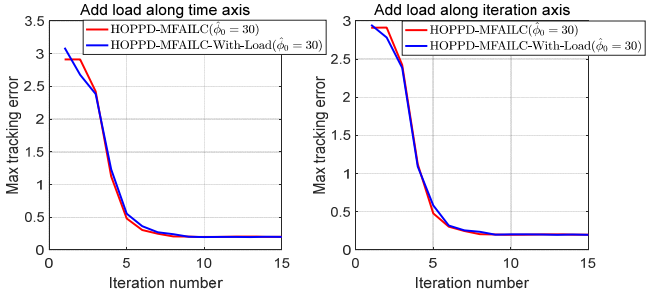

Fig. 13. Comparison of maximum tracking errors of HOPPD-MFAILC with load-free and load-added along time axis or iteration axis.

Finally, experiments on tracking the desired trajectory in simulation are conducted to make the calculation result and experimental result correspond with each other. The desired trajectory of PAM is set to be the same as the simulation trajectory in (31). Fig. 14 shows the tracking result of PAM controlled by MFAILC and HOPPD-MFAILC with $\hat{\phi}_0 = 40$. It reveals that with the increase of iterations, the actual trajectory of the PAM gradually approaches the desired one, though there are certain unavoidable overshoots in real-world due to the step response. Comparing (a) with (b) in Fig. 14, it is obvious that the HOPPD-MFAILC method can track the desired trajectory more quickly within 9 iterations. We can conclude that the PAM controlled by HOPPD-MFAILC is able to track the desired trajectory in better performance after several iterations and this is in consistent with the theory and the simulation. Though there are some delays in practical tests due to the memory-based scheme, the control signals of previous trials can be manipulated at a time ahead of the current instance, which means we can compensate the process or time delay.

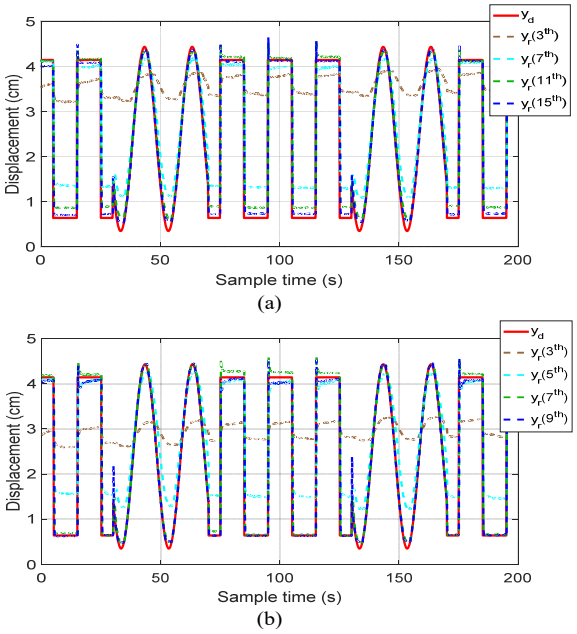

Fig. 14. Tracking results of PAM controlled by (a) MFAILC and (b) HOPPD-MFAILC with $\hat{\phi}_0 = 40$ for the trajectory in simulation.

To statistically compare the different experiments mentioned above, the maximum tracking errors and the root mean square (RMS) errors of MFAILC and HOPPD-MFAILC schemes under different PPDs are calculated. The maximum tracking error and RMS error of HOPPD-MFAILC method at different frequencies and different starting iterations are also obtained respectively. Finally, the results are compared between controls without and with loads added along the time axis and along the iteration axis. The calculated results are shown in Table I. Statistical results show that different initial PPDs will greatly affect the convergence of MFAILC, while HOPPD-MFAILC can always maintain a good performance. For example, the maximum tracking error of HOPPD-MFAILC is about 0.2 at the 9th iteration, while the maximum errors of MFAILC are greatly affected by the initial PPDs, resulting 0.1830, 0.2357, 0.3602, and 0.5051, respectively with different PPDs. Control performance of the proposed method does not change much at

different frequencies and with or without load interferences, which validate its good robustness. The convergence speed is quite different when start using the high-order estimation algorithm from different iterations, which means the earlier we use it the better convergence we can achieve. For example, the maximum tracking error of the ninth iteration is 0.1474 when the higher order estimation algorithm is used from the fourth iteration, and 0.3196 and 0.4866 when the algorithm is used from the eighth and the twelfth iteration, respectively. These all prove that the proposed method can improve the convergence rate and obtain an overall better control performance.

TABLE I
QUANTITATIVE COMPARISON OF EXPERIMENTAL RESULTS

Iteration number		Maximum tracking error			RMS error		
		3	5	9	3	5	9
MFACILC (f =0.5Hz)	$\hat{\phi}_0 = 10$	1.1080	0.2581	0.1830	0.6671	0.1046	0.0683
	$\hat{\phi}_0 = 20$	2.0540	0.4954	0.2375	1.1140	0.3127	0.0686
	$\hat{\phi}_0 = 30$	2.4860	0.9972	0.3602	1.3460	0.5773	0.1678
	$\hat{\phi}_0 = 40$	2.7470	1.4510	0.5051	1.4960	0.8157	0.2838
HOPPD-MFAILC (f =0.5Hz)	$\hat{\phi}_0 = 10$	1.1080	0.2633	0.1811	0.6671	0.1296	0.0633
	$\hat{\phi}_0 = 20$	2.0090	0.3635	0.2033	1.1010	0.2011	0.0634
	$\hat{\phi}_0 = 30$	2.4220	0.4795	0.2054	1.3170	0.2846	0.0697
	$\hat{\phi}_0 = 40$	2.6440	0.8222	0.2066	1.4380	0.4937	0.0713
HOPPD-MFAILC ($\hat{\phi}_0 = 40$)	f =0.5Hz	2.6440	0.8222	0.2066	1.4380	0.4937	0.0713
	f =2.5Hz	2.5410	0.8207	0.1524	1.3880	0.4770	0.0402
	f =5Hz	2.6050	0.8276	0.1867	1.4230	0.4871	0.0619
HOPPD-MFAILC ($\hat{\phi}_0 = 40$)	k =4	2.4860	0.7659	0.1474	1.3600	0.4774	0.0421
	k =8	2.3800	1.3350	0.3196	1.3250	0.7682	0.1725
	k =12	2.4600	1.3460	0.4866	1.3490	0.7740	0.2720
HOPPD-MFAILC with loads	in time axis	2.3850	0.5545	0.1974	1.3810	0.3480	0.1008
	in iterations	2.3850	0.5831	0.1973	1.3020	0.3385	0.0781

IV. DISCUSSION AND CONCLUSION

In this paper, a high-order parameter estimation based model-free adaptive iterative learning controller is proposed for PAM. HOPPD-MFAILC is a completely model-free adaptive method that just utilizes input and output data of the nonlinear system. The dynamic linearization method is introduced to establish the data model along the iteration axis, in which the PPD is determined by the improved high-order estimation algorithm. The main advantage of HOPPD- MFAILC relies on its ability to use the data in previous iterations, speed up the estimation of parameters, and improve the convergence while ensuring the control accuracy. Both simulation and PAM control experiment results show that the proposed HOPPD-MFAILC has a faster convergence speed than MFAILC and is more suitable for nonlinear systems. The tracking errors of the proposed method did not show significant improvement over MFAILC or some other iterative learning control methods such as [29-31]. In these studies, the maximum errors ranged from 6% to 10% [29-31], while the error of the proposed method is about 7% after tuned. One reason is that most of the current controllers were implemented on rigid motors, as we know the PAM has compliant features but the drawback is its control accuracy, so the results in this work are fairly satisfactory. Even so, the main contribution of our work is to propose a HOPPD-MFAILC method with faster convergence speed. From Fig. 4, Fig. 11, and Fig. 14, we can see that both methods can converge to a low error level, but the convergence of the proposed method is more efficient, which shows its superior convergence performance over MFAILC and other methods, since it can reach the stable state within 7 or 8 iterations while other control approaches need more times, such as 15 iterations in [30], and over 20 iterations in [29, 31]. Consequently, the theoretical proof, simulation and experiment results all prove that the proposed method has a faster convergence speed.

For real-time issues, ILC is a memory-based mechanism and the memory devices are extremely cheap and easily accessible with the present technology [32]. Our work is to propose a high-order pseudo-partial derivative based model-free adaptive ILC, which fully utilizes the input/output data in previous iterations during the control process. Though the learning control methods require a memory to store the data, since the feedback configuration can give additional advantages such as enhanced convergence rate [33], they in turn make the control straightforwardly. Moreover, the record of data in several previous iterations will not affect the real-time performance as the current technology is able to handle the data of this level almost in real-time [34]. From the experiment results, we can also confirm that the proposed controller can be optimized in an almost real-time fashion during operations, and the real-time performance is improved as compared with other gradient-descent-type methods such as iterative feedback tuning that may suffer from the drawback of slow convergence [15].

In the future, the proposed method will be implemented on the PAMs-driven ankle rehabilitation robot and new tuning methods will be investigated to further improve the adaptability and robustness of the controller for human robot interaction. Further, the human voluntary movement is not the only factor that may affect the rehabilitation performance, muscle fatigue, emotion and other factors also play important roles during the rehabilitation [6]. Patient's recovery can be comprehensively evaluated from the recorded physiological data, based on which more reasonable adjustment of the robot assistance will be proposed to improve the rehabilitation effectiveness [35].

REFERENCES

[1] G. Andrikopoulos, G. Nikolakopoulos, I. Arvanitakis, and S. Manesis, "Piecewise affine modeling and constrained optimal control for a pneumatic artificial muscle," *IEEE Trans. Ind. Electron.,* vol. 61, pp. 904-916, 2013.

[2] D. Zhang, X. Zhao, and J. Han, "Active model based control for pneumatic artificial muscle," *IEEE Trans. Ind. Electron.,* vol. 64, pp. 1686-1695, 2017.

[3] J. Huang, X. Tu, and J. He, "Design and evaluation of the RUPERT wearable upper extremity exoskeleton robot for clinical and in-home therapies," *IEEE Trans. Syst. Man Cybern.,* vol. 46, pp. 926-935, 2016.

[4] G. Sawicki and D. Ferris, "A pneumatically powered knee-ankle-foot orthosis (KAFO) with myoelectric activation and inhibition," *J. Neuroeng. Rehabil.,* vol. 6 (23), pp. 1-16, 2009.

[5] K. Knaepen, A. Mierau, E. Swinnen, H. F. Tellez, M. Michielsen, E. Kerckhofs, *et al.*, "Human-robot interaction: does robotic guidance force affect gait-related brain dynamics during robot-assisted treadmill walking?," *PLoS One,* vol. 10, p. e0140626, 2015.

[6] V. Klamroth-Marganska, J. Blanco, K. Campen, A. Curt, V. Dietz, T. Ettlin, *et al.*, "Three-dimensional, task-specific robot therapy of the arm after stroke: a multicentre, parallel-group randomised trial," *Lancet Neurol.,* vol. 13, pp. 159-166, 2014.

[7] Q. Ai, C. Zhu, J. Zuo, W. Meng, Q. Liu, *et al.*, "Disturbance-estimated adaptive backstepping sliding mode control of a pneumatic muscles-driven ankle rehabilitation robot," *Sens.,* vol. 18(66), pp. 1-21, 2018.

[8] M. Zhang, S. Q. Xie, X. Li, G. Zhu, W. Meng, X. Huang, and A. J. Veale, "Adaptive patient-cooperative control of a compliant ankle rehabilitation robot (CARR) with enhanced training safety," *IEEE Trans. Ind. Electron.*, vol. 65, pp.1398-1407, 2018.

[9] B. Yao, Z. Zhou, Q. Liu, and Q. Ai, "Empirical modeling and position control of single pneumatic artificial muscle," *Control Eng. Appl. Inf.,* vol. 18, pp. 86-94, 2016.
[10] X. Zang, Y. Liu, S. Heng, Z. Lin, and J. Zhao, "Position control of a single pneumatic artificial muscle with hysteresis compensation based on modified Prandtl-Ishlinskii model," *Bio-Med. Mater. Eng.,* vol. 28, pp. 131-140, 2017.
[11] S. Chakraborty and N. Zabaras, "Efficient data-driven reduced-order models for high-dimensional multiscale dynamical systems," *Comput. Phys. Commun.,* vol. 230, pp. 70-88, 2018.
[12] Y. Xie, X. Tang, W. Meng, B. Ye, B. Song, J. Tao, *et al.*, "Iterative data-driven fractional model reference control of industrial robot for repetitive precise speed-tracking," *IEEE/ASME Trans. Mechatron.,* vol. 99, pp. 1-12, 2019.
[13] F. Song, Y. Liu, J. Xu, X. Yang, and Q. Zhu, "Data-driven iterative feedforward tuning for a wafer stage: A high-order approach based on instrumental variables," *IEEE Trans. Ind. Electron.,* vol. 66, pp. 3106-3116, 2018.
[14] Z. Hou and S. Jin, *Model Free Adaptive Control: Theory and Applications*, CRC Press, Boca Raton, 2013.
[15] W. Meng, S. Xie, Q. Liu, C. Lu, and Q. S. Ai, "Robust iterative feedback tuning control of a compliant rehabilitation robot for repetitive ankle training," *IEEE/ASME Trans. Mechatron.,* vol. 22, pp. 173-184, 2017.
[16] D. Ke, Q. Ai, W. Meng, C. Zhang, and Q. Liu, "Fuzzy PD-type iterative learning control of a single pneumatic muscle actuator," in *Int. Conf. Intell. Rob. Appl.*, vol. 10463, Wuhan, China, pp. 812-822, 2017.
[17] Y. Cui, T. Matsubara, and K. Sugimoto, "Pneumatic artificial muscle-driven robot control using local update reinforcement learning," *Adv. Rob.,* vol. 31, pp. 397-412, 2017.
[18] Z. Hou, R. Chi, and H. Gao, "An overview of dynamic linearization based data-driven control and applications," *IEEE Trans. Ind. Electron.,* vol. 64, pp. 4076-4090, 2017.
[19] R. Chi, Adaptive Iterative Learning Control for Nonlinear Discrete-Time Systems and Its Applications, Beijing Jiaotong University, 2006.
[20] R. Chi, Z. Hou, S. Jin, and B. Huang, "Computationally efficient data-driven higher order optimal iterative learning control," *IEEE Trans. Neural Networks Learn. Syst.,* vol. 29, pp. 5971-5980, 2018.
[21] X. Bu, Q. Yu, Z. Hou, and W. Qian, "Model free adaptive iterative learning consensus tracking control for a class of nonlinear multiagent systems," *IEEE Trans. Syst. Man Cybern.,* vol. 49, pp. 677-686, 2017.
[22] B. Luo, H. N. Wu, and T. Huang, "Optimal output regulation for model-free Quanser helicopter with multistep Q-learning," *IEEE Trans. Ind. Electron.,* vol. 65, pp. 4953-4961, 2017.
[23] Z. Hou and Y. Zhu, "Controller-dynamic-linearization-based model free adaptive control for discrete-time nonlinear systems," *IEEE Trans. Ind. Inf.,* vol. 9, pp. 2301-2309, 2013.
[24] Z. Hou, J. Xu, "On data-driven control theory: the state of the art and perspective," *Acta Autom. Sin.,* vol. 35, pp. 650-667, 2009.
[25] B. Chu, D. H. Owens, and C. T. Freeman, "Iterative learning control with predictive trial information: convergence, robustness, and experimental verification," *IEEE Trans. Control Syst. Technol.,* vol. 24, pp. 1101-1108, 2015.
[26] R. Chi, B. Huang, Z. Hou, and S. Jin, "Data-driven high-order terminal iterative learning control with a faster convergence speed," *Int. J. Robust Nonlinear Control,* vol. 28, pp. 103-119, 2017.
[27] R. Chi, Y. Liu, Z. Hou, and S. Jin, "Data-driven terminal iterative learning control with high-order learning law for a class of non-linear discrete-time multiple-input–multiple output systems," *IET Control Theory Appl.,* vol. 9, pp. 1075-1082, 2015.
[28] X. Wang, B. Chu, and E. Rogers, "Repetitive process based higher-order iterative learning control law design," in *2016 Am. Control Conf. (ACC)*, pp. 378-383, 2016.
[29] X. Zhu, J. Wang, and X. Wang, "Nonlinear iterative learning control of 5 DOF upper-limb rehabilitation robot," in *IEEE Int. Conf. Rob. Biomimetics*, Zhuhai, China, pp. 793-798, 2015.
[30] C. Guo, S. Guo, J. Ji, and F. Xi, "Iterative learning impedance for lower limb rehabilitation robot," *J. Healthcare Eng.,* vol. 2017, pp. 1-9, 2017.
[31] P. Sampson, C. Freeman, S. Coote, S. Demain, *et al.*, "Using functional electrical stimulation mediated by iterative learning control and robotics to improve arm movement for people with multiple sclerosis," *IEEE Trans. Neural Syst. Rehabil. Eng.,* vol. 24, pp. 235-248, 2016.
[32] J. X. Xu, S. K. Panda, and T. H. Lee, *Real-Time Iterative Learning Control: Design and Applications*: Springer-Verlag London, 2009.
[33] I. Chin, S. J. Qin, K. S. Lee, and M. Cho, "A two-stage iterative learning control technique combined with real-time feedback for independent disturbance rejection," *Autom.,* vol. 40, pp. 1913-1922, 2004.
[34] T. W. Chow and Y. Fang, "A recurrent neural-network-based real-time learning control strategy applying to nonlinear systems with unknown dynamics," *IEEE Trans. Ind. Electron.,* vol. 45, pp. 151-161, 1998.
[35] C. Shirota, J. Jansa, J. Diaz, S. Balasubramanian, S. Mazzoleni, N. A. Borghese, *et al.*, "On the assessment of coordination between upper extremities: towards a common language between rehabilitation engineers, clinicians and neuroscientists," *J. NeuroEng. Rehabil.,* vol. 13 (80), pp. 1-14, 2016.

Qingsong Ai (M'19) received the Ph.D. degree in information engineering from Wuhan University of Technology, China, in 2008. He was a visiting researcher at the University of Auckland, New Zealand (2006-2007) and at the University of Leeds, UK (2017-2018). He is currently a full Professor at the Wuhan University of Technology. Prof. Ai is the project leader of 12 national, ministerial or provincial projects with the total amount of 13M RMB. He has published over 70 international journal papers, book chapters and conference papers.

Da Ke and **Jie Zuo** are a Master student and a Ph.D. student at School of Information Engineering, Wuhan University of Technology.

Wei Meng (M'17) received the Ph.D. degree in information and mechatronics engineering jointly trained by Wuhan University of Technology, China and the University of Auckland, New Zealand in 2016. He is currently with the School of Information Engineering, Wuhan University of Technology, China and a Research Fellow at the School of Electronic and Electrical Engineering, University of Leeds, UK. He has authored/co-authored 3 books and over 50 peer-reviewed papers in rehabilitation robotics and control.

Quan Liu received the Ph.D. degree in mechanical engineering in 2003 from Wuhan University of Technology, China, where she is currently a Chair Professor in information science. She has authored over 100 academic papers and books and directed over 20 research projects. Her research interests include signal processing, embedded systems, robots and electronics. Prof. Liu obtained 2 national awards and 3 provincial and ministerial awards. She is the Council Member of Chinese Association of Electromagnetic Compatibility and the Hubei Institute of Electronics.

Zhiqiang Zhang is a University Academic Fellow (UAF) in body sensor networks for healthcare and robotic control at the University of Leeds. He has pioneered research into human kinematics, musculoskeletal modeling and machine learning. He has >50 papers in peer reviewed publications, and has been nominated for the best paper awards at the International Conference on Body Sensor Networks (BSN) in 2010, 2011 and 2014.

Sheng Q. Xie (SM'11) received the Ph.D. degree in mechanical engineering from the University of Canterbury, New Zealand, in 2002. He joined the University of Auckland in 2003 and became a Chair Professor in (bio)mechatronics in 2011. Since 2017 he has been the Chair in Robotics and Autonomous Systems at the University of Leeds. He has authored or coauthored 8 books, 15 book chapters, and over 400 international journal and conference papers. His current research interests are medical and rehabilitation robots, advanced robot control. Prof. Xie is an elected Fellow of The Institution of Professional Engineers New Zealand (FIPENZ).